Emission line of galaxies (II) : classification

Shiyin Shen

BPT diagram

always one of the following: (a) photoionization by O and B stars, (b) photoionization by a power-law continuum source, or (c) shock-wave heating. A fourth excitation class is the planetary nebulae, which are photo-

- Baldwin, Phillips, & Terlevich (1981)

+: PN
X: Shock-heated
Diamond: AGN

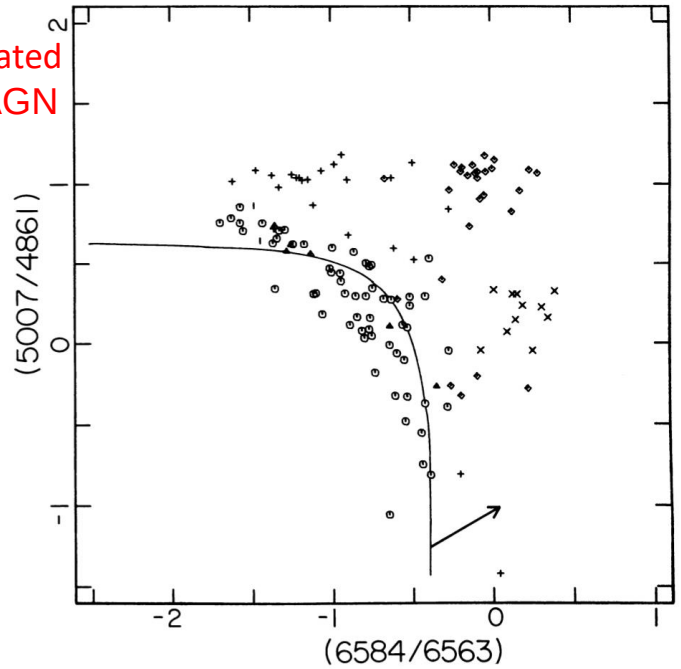

V=VI+VII: Balmer lines
VI: low ionization region: O+ N+ ions
VII: high ionization region:O++ ions

$$I(\mathrm{H}\beta) \propto I(\mathrm{H}\alpha\ \lambda6563) \propto N_e^2\, V \ ,$$

$$I([\mathrm{O\ II}]\ \lambda3727) \propto I([\mathrm{N\ II}]\ \lambda6584) \propto N_e^2\, V_{\mathrm{I}} \ ,$$

and

$$I([\mathrm{O\ III}]\ \lambda5007) \propto N_e^2\, V_{\mathrm{II}} \ .$$

- Osterbrock & de Robertis (1985)
- Veilleux & Osterbrock (1987).

Veilleux & Osterbrock 1987

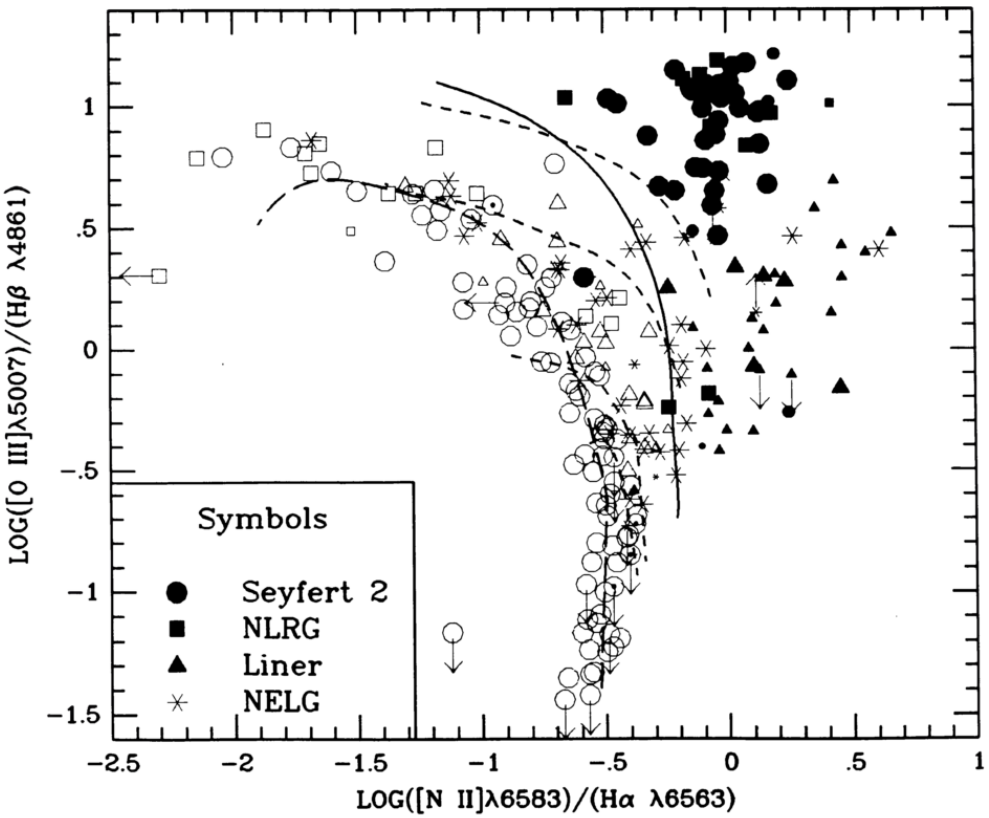

Four short-dashed lines are H n region models of Evans and Dopita (1985) for T* = 56,000, 45,000, 38,5000, and 37,000 K from the top to bottom respectively.

The number of photons capable of ionizing O+ depends on U and T*; it decreases as we progress from high to low U and T*. Consequently, the size of the O++ zone and the total [OIII] emission also decrease. For a given T*, as U decreases, the zone containing a singly ionized species such as N+ therefore becomes steadily larger and eventually fills the whole volume of the ionized H+ zone.

It is necessary to assume an anticorrelation between ionization parameter and metallicity. On this picture for large U the metallicity is smaller than the solar value, the line opacity in the model stellar atmospheres is less efficient, and hence there are more far-ultraviolet photons, resulting in a larger 0++ zone and a smaller N+ zone.

Kewley （2001）

theoretical upper limit for HII regions

$(Z = 0.1\text{–}3.0)$ and ionization parameter q (cm s^{-1}) in the range $5 \times 10^6 \leq q \leq 3 \times 10^8$ (or $-3.5 \leq \log \mathscr{U} \leq -2.0$),

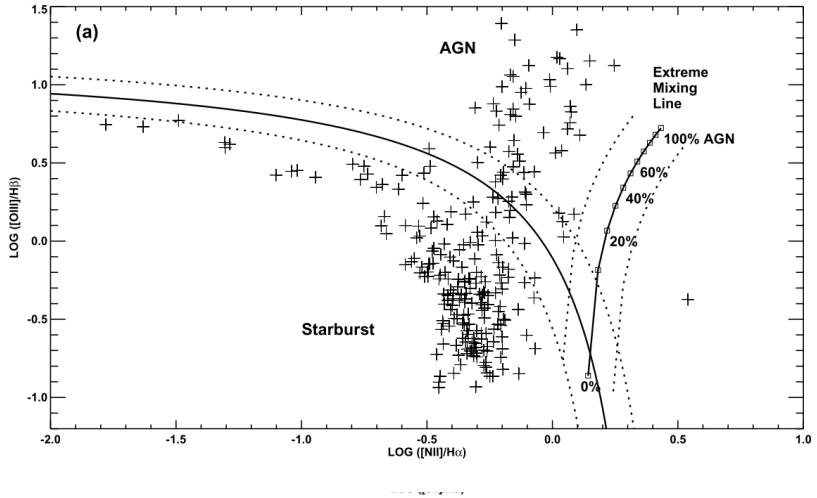

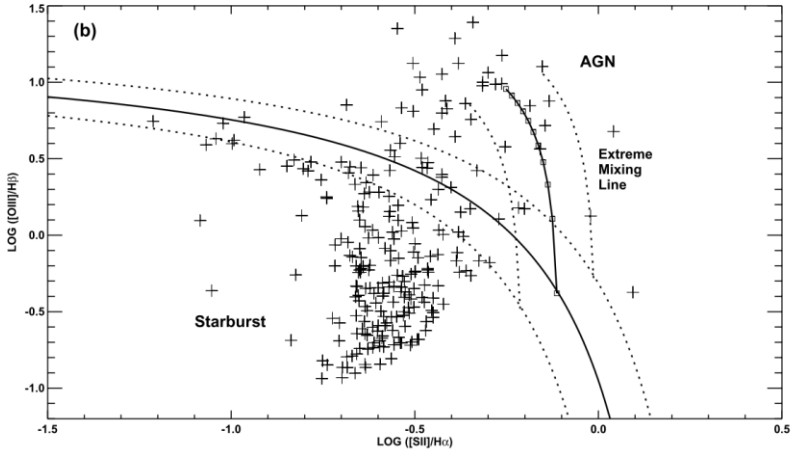

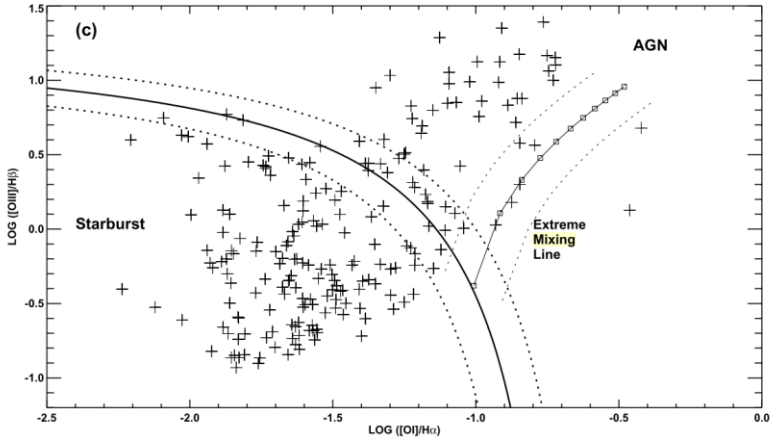

$$\log\left(\frac{[\text{O III}]\ \lambda 5007}{\text{H}\beta}\right) = \frac{0.61}{\log\left([\text{N II}]/\text{H}\alpha\right) - 0.47} + 1.19\,, \quad ($$

$$\log\left(\frac{[\text{O III}]\ \lambda 5007}{\text{H}\beta}\right) = \frac{0.72}{\log\left([\text{S II}]\ \lambda\lambda 6717, 31/\text{H}\alpha\right) - 0.32} + 1.30\,, \quad ($$

$$\log\left(\frac{[\text{O III}]\ \lambda 5007}{\text{H}\beta}\right) = \frac{0.73}{\log\left([\text{O I}]\ \lambda 6300/\text{H}\alpha\right) + 0.59} + 1.33\,. \quad ($$

Kauffmann et al. 2003

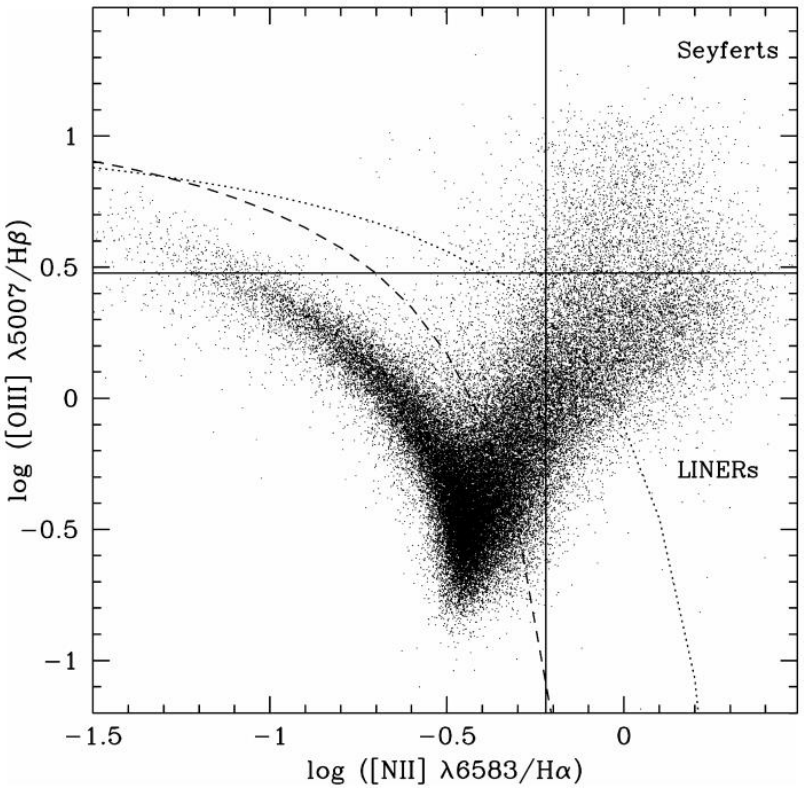

- Empirical relation from large sample of SDSS galaxies
  - Aperture effect

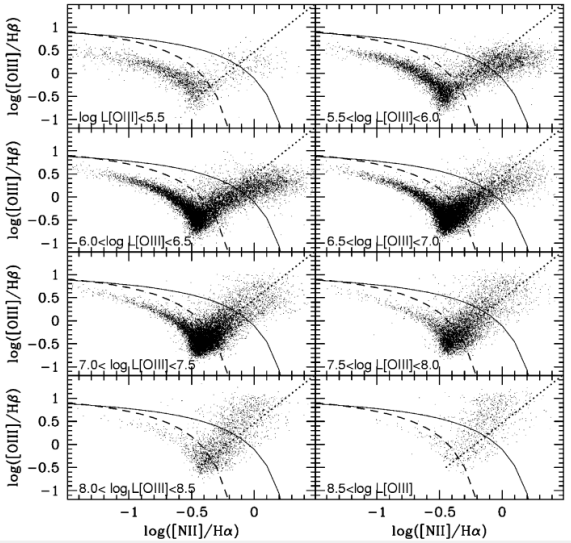

$$\log([\mathrm{O\,III}]/\mathrm{H}\beta) > 0.61/\{\log([\mathrm{N\,II}]/\mathrm{H}\alpha) - 0.05\} + 1.3.$$

Kewley et al. 2006

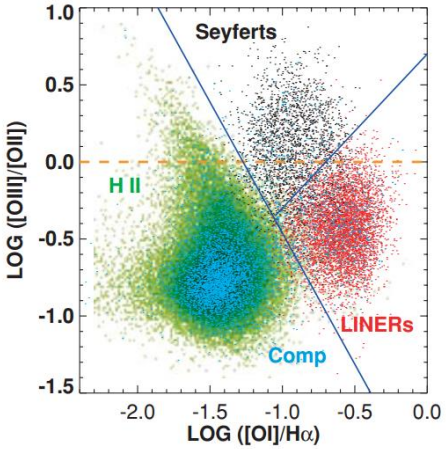

- six lines
  - 5 classes
  - star-forming galaxies(75%), Seyferts(3%), LINERs(7%) , composites(7), ambiguous galaxies (8 per cent).

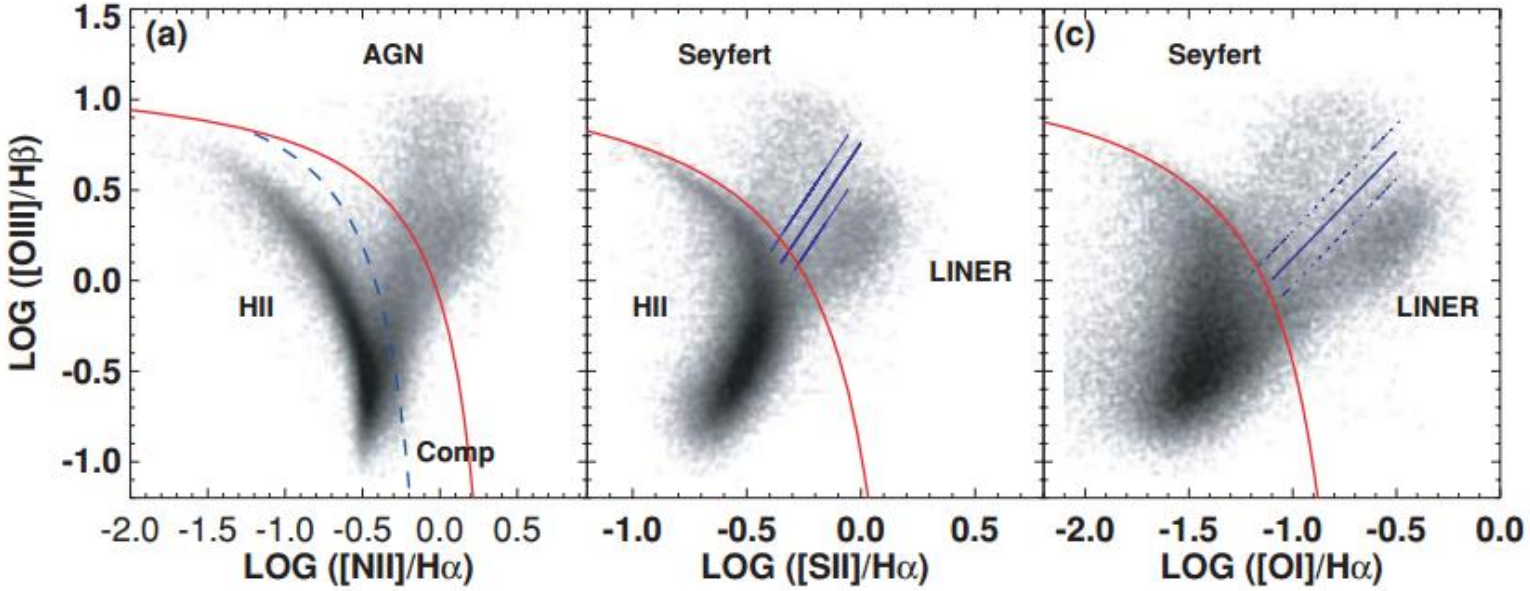

Stasińska et al. 2006

Why BPT the best

- At metallicities larger than about 0.3 Zsun, N/O increases with O/H

NII and Ha only

$$\log[\mathrm{N\,II}]/\mathrm{H}\alpha \leqslant -0.4 \quad \text{NSF},$$
$$-0.4 < \log[\mathrm{N\,II}]/\mathrm{H}\alpha \leqslant -0.2 \quad \text{hybrid},$$
$$\log[\mathrm{N\,II}]/\mathrm{H}\alpha > -0.2 \quad \text{AGN}.$$

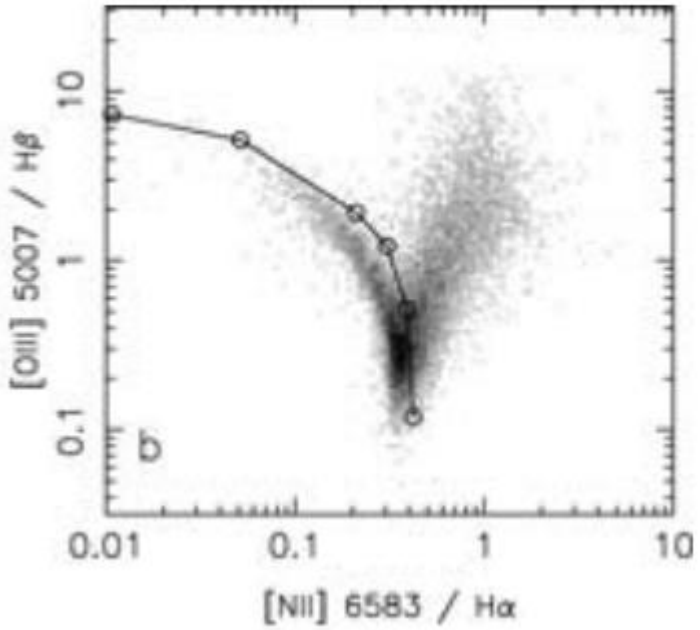

理论线，比K03更靠下

DEW, useful to high z

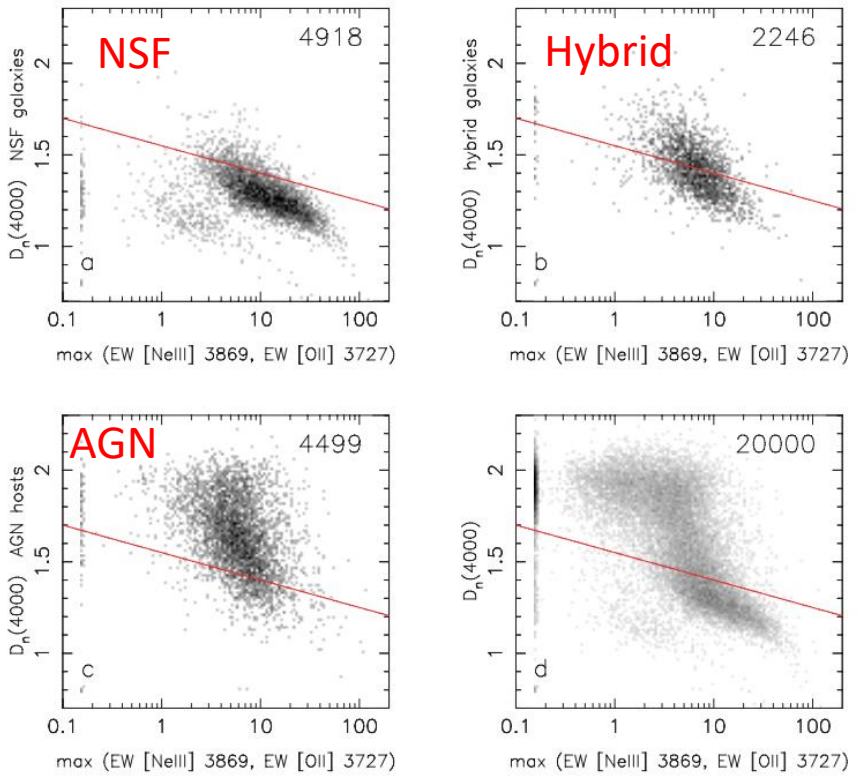

WHAN diagram (Cid Fernandes 2010)

- ~%43 SDSS galaxies with four BPT lines detected with S/N>3 (Hb is weak!)
  - ~75 with Ha and [NII] detected with S/N>3

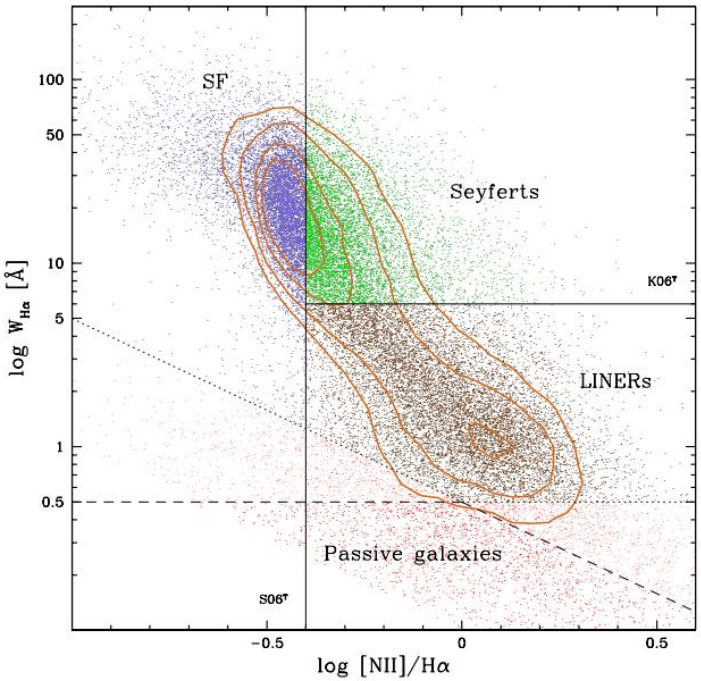

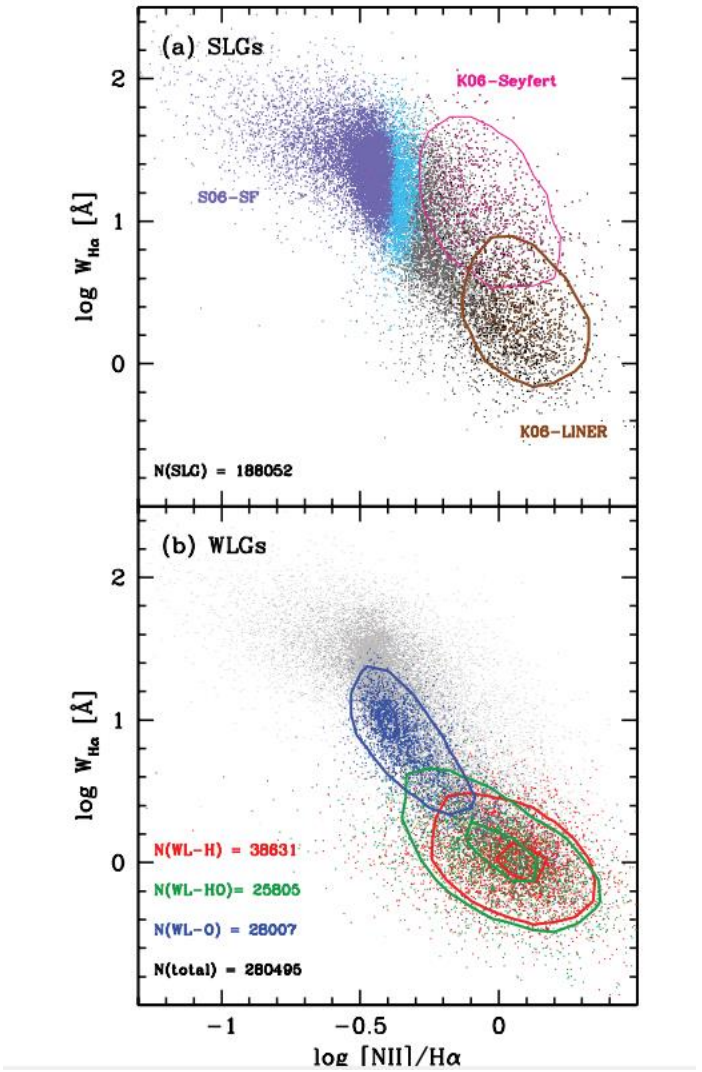

Discussion (Cid Fernandes 2010)

- The K01 ‘extreme starburst’ line in the BPT plane was obtained by considering the upper envelope of model nebulae ionized by massive stars. Hence, according to the K01 models, sources currently classified as composites (i.e. between the K01 and K03 lines) do not require the presence of an AGN, and, conversely, locations above the ‘extreme starburst’ line may well be reached by composite SF+AGN systems. The K01 line in the BPT plane was never intended to trace the frontier of ‘pure AGN’, as it is used nowadays.
- Photoionization models with either a pure AGN(Stasinska 1984) or a purely old stellar population (Stasinska et al. 2008) are able to cover the region between the K03 and K01 lines without mixing massive stars and AGN at all.
- All in all, the use of the term ‘composite’ to denote objects between the K01 and K03 lines is misleading, even if part of the galaxies in this zone is indeed mixtures of SF and AGN. If anything, such sources should be called ‘intermediate’, i.e. in between the bottom and the tip of the right wing.
- The K03 line is somewhat arbitrary at the bottom of the BPT diagram. S06 produced a more stringent line which follows more closely the upper envelope of the bulk of SF galaxies and was extrapolated to the ‘body’ of the seagull, where the left and right wings meet and no clear frontier is seen. This extrapolation was achieved by means of photoionization models, and may obviously be wrong, but it is, for the moment, the best available

WHAN diagram (Cid Fernandes 2011)

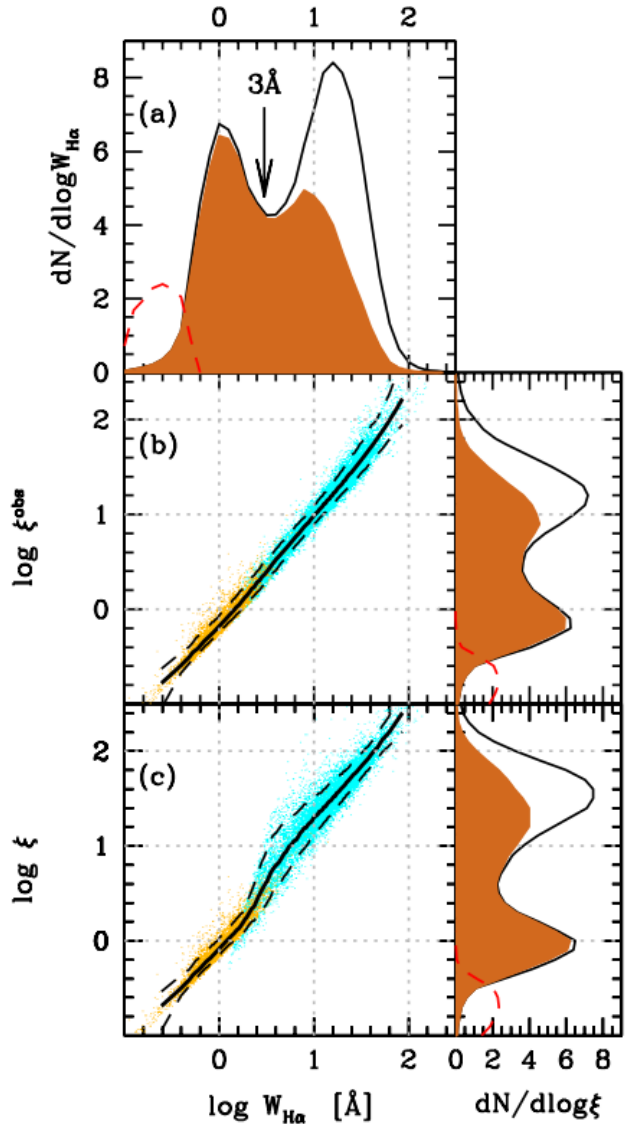

RGs are systems whose old stellar populations suffice to explain the observed emission line properties.

$$\xi = \frac{L_{H\alpha}^{int}}{L_{H\alpha}^{exp}(t > 10^8\ yr)}$$

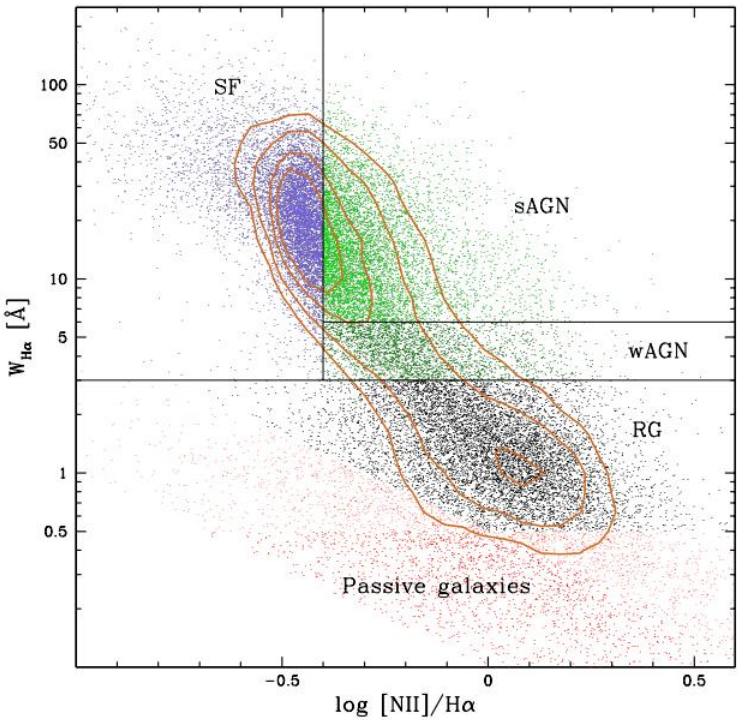

Star formation history

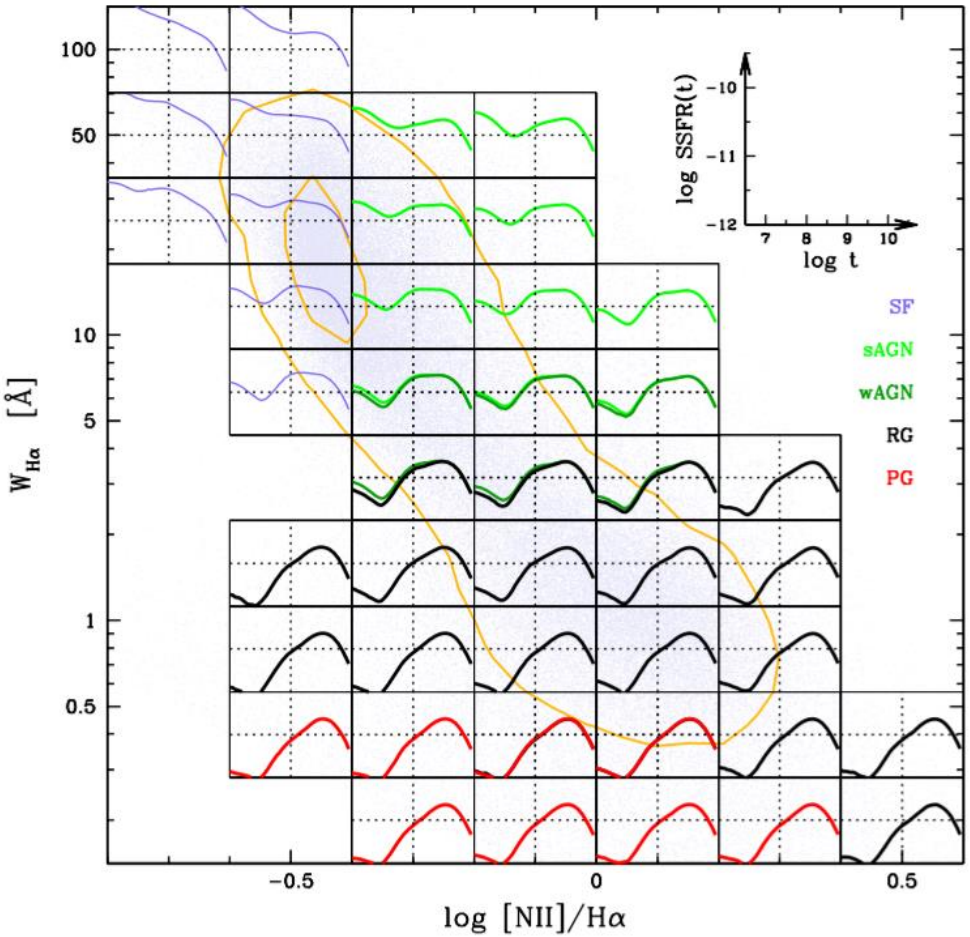

Probabilistic approach(de Souza et al. 2017)

- Gaussian mixture model(GMM)
  - 4 Gaussian components, 97% data variance
    - GC1 and GC4: star forming
    - GC2: AGN(BPT) & weak AGN(WHAN)
    - GC3: composite(BPT) & strong AGN(WHAN)

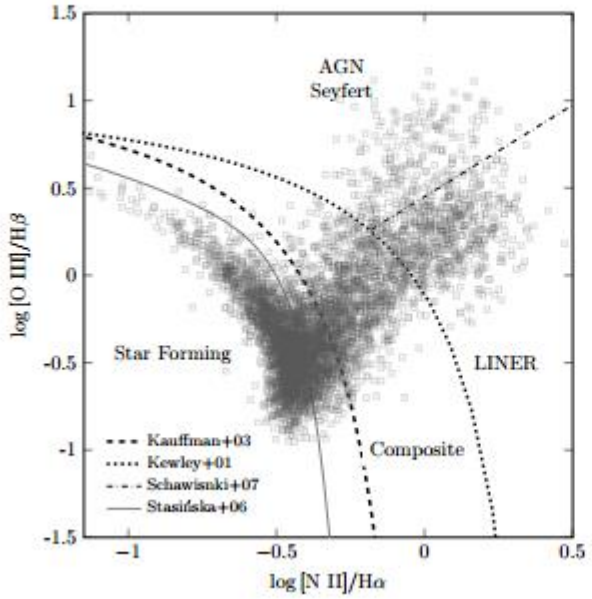

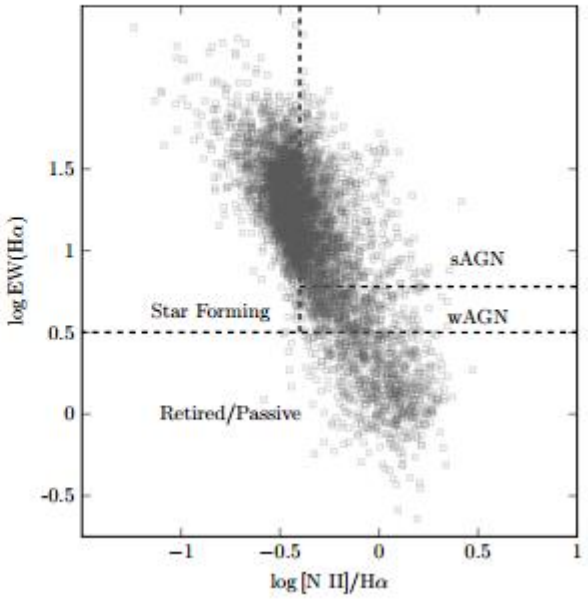

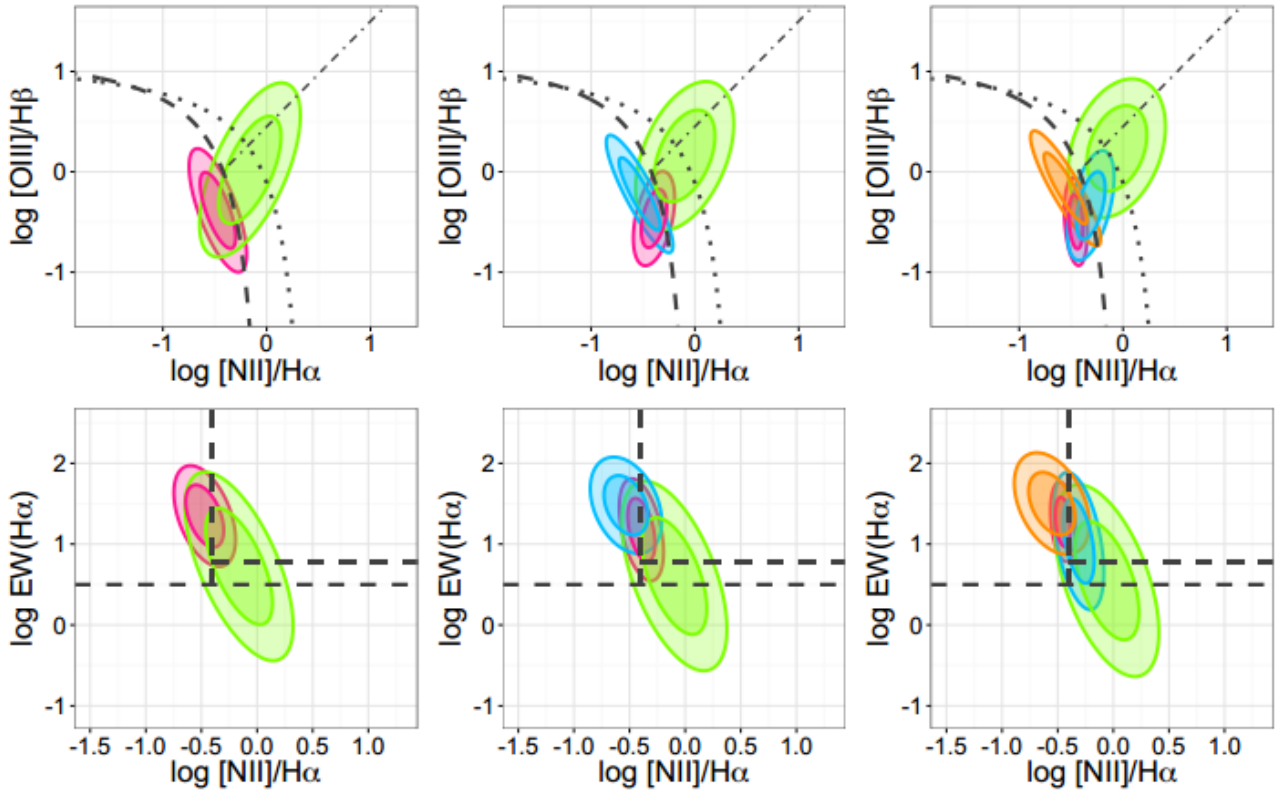

Figure 2. The Gaussian components projected onto the BPT (top panels) and WHAN (bottom panels) diagrams. From left to right are the solutions for 2, 3 and 4 GCs. For each component the thick lines represent 68% and 95% confidence levels, respectively.

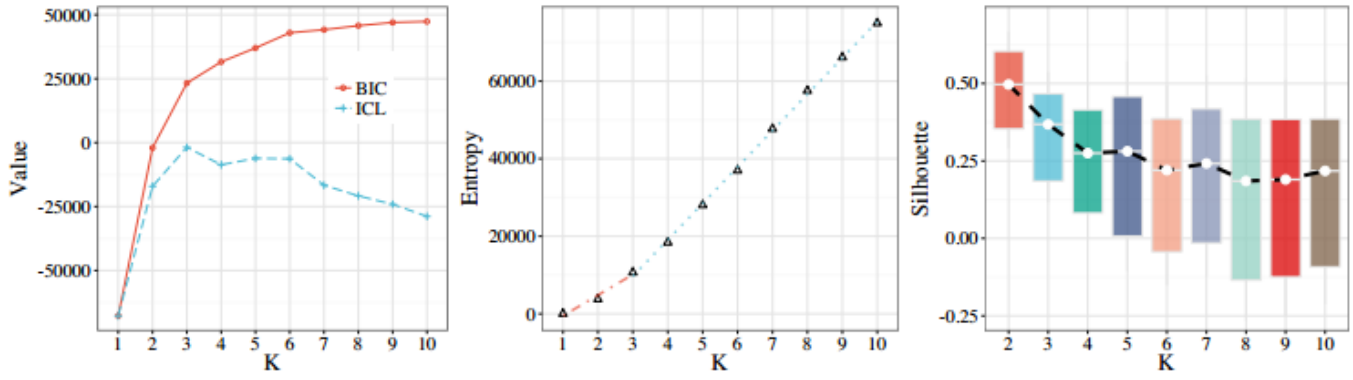

LINER → LIER (Belfior et al. 2016)

- low ionisation nuclear emission line regions LINERs, (Heckman 1980)
- low ionisation emission-line regions (LIERs)

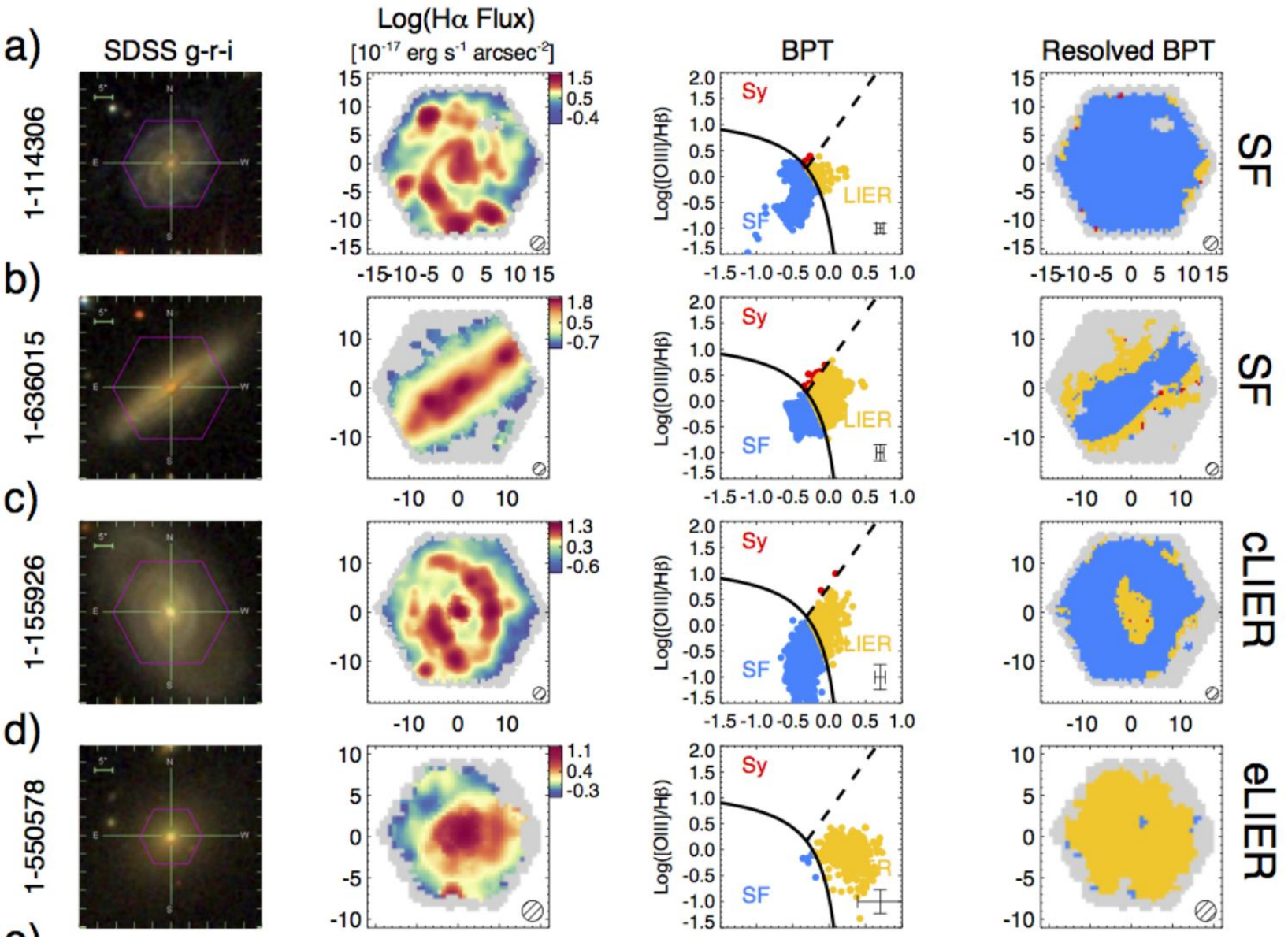
a)
b)
c)
d)
1-114306
1-636015
1-155926
1-550578
SDSS g-r-i
Log(Hα Flux)
[10^-17 erg s^-1 arcsec^-2]
BPT
Resolved BPT
Sy
LIER
SF
Log([OIII]/Hβ)
SF
SF
cLIER
eLIER

Age sequence?

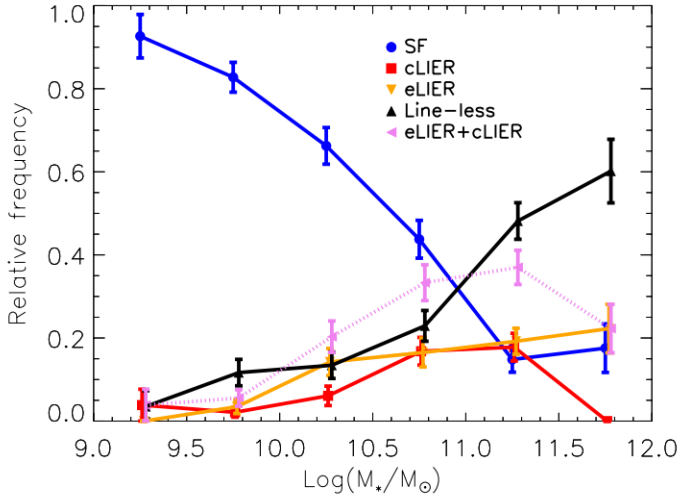

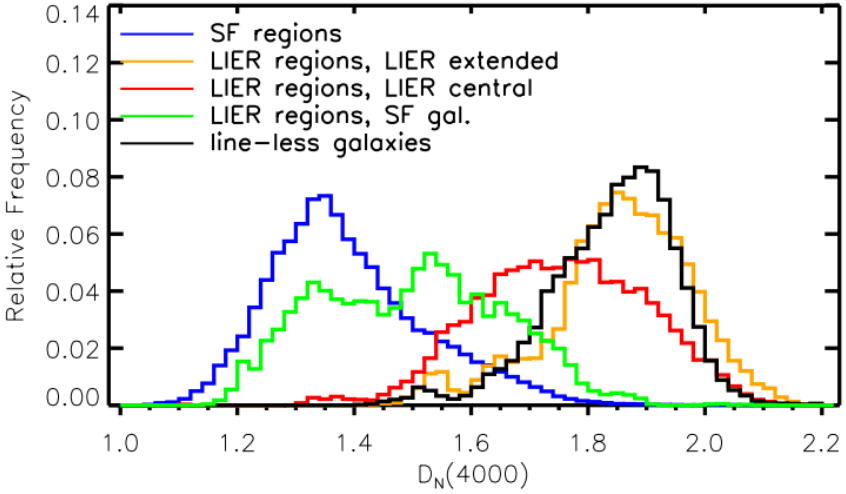

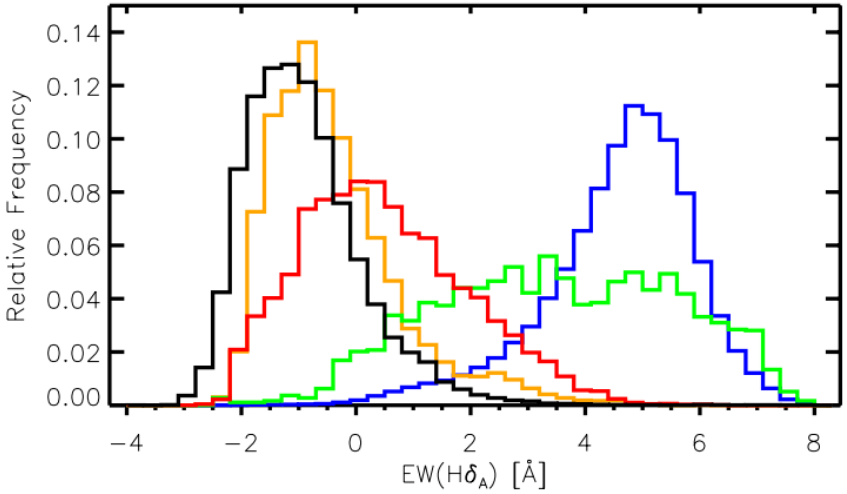

LINER? (Heckman & Best 2014)

- Many studies have all presented evidence that those LINERs with the weakest emission lines are not powered by an AGN. Instead, most of these papers argue that they are produced by photoionization of neutral atomic gas by a population of post-asymptotic giant branch (PAGB) stars.
- A problem with this idea is that Hubble Space Telescope (HST)UV images of the bulge of M31 (the site of a LINER) do not reveal the predicted population of these PAGBstars (Brown et al. 1998, 2008; Rosenfield et al. 2012).
- For these weak LINERs to be photoionized by old stars, a population that is less luminous and more numerous than the PAGB stars would be needed.
- Here we consider weak LINERs to be objects with [OIII]5007 equivalent widths smaller than $\sim$1A$^{\circ}$ (e.g., Capetti & Baldi 2011). It is important to note that although these objects constitute the majority of LINERs in the SDSS, they contribute a negligible amount to the overall AGN emissivity of the contemporary Universe.
- It is also important to note that objects classified as LINERs in the SDSS span over two orders of magnitude in [OIII] luminosity (L[OIII]) and roughly three orders of magnitude in L[OIII]/MBH.
- Although a stellar origin for the LINER emission is likely at the lowest luminosities, the more powerful LINERs are most likely to be AGNs.

Mergers: shocks

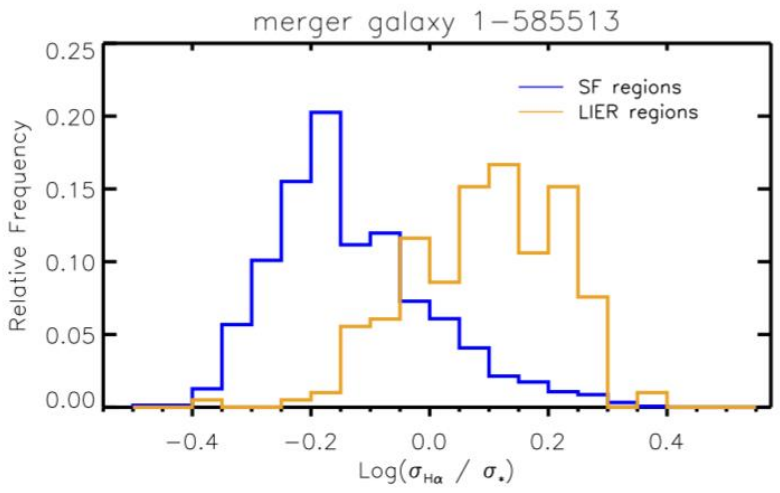

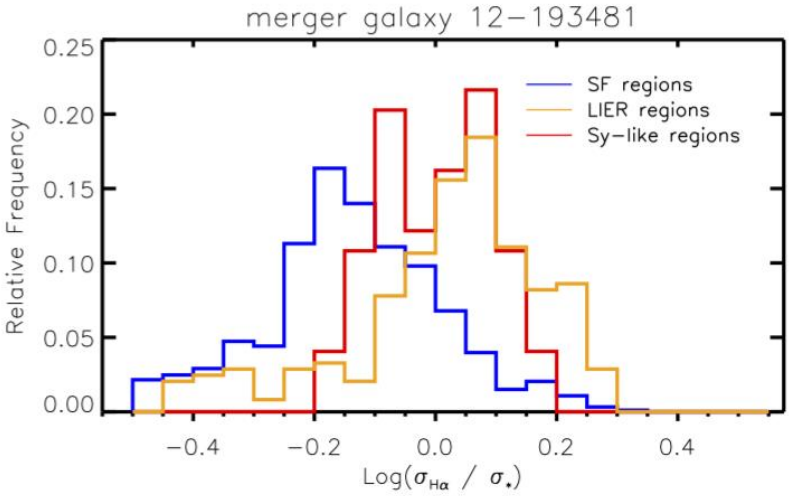

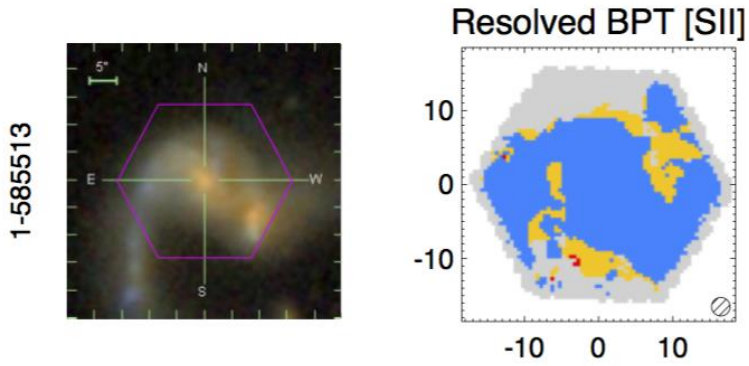

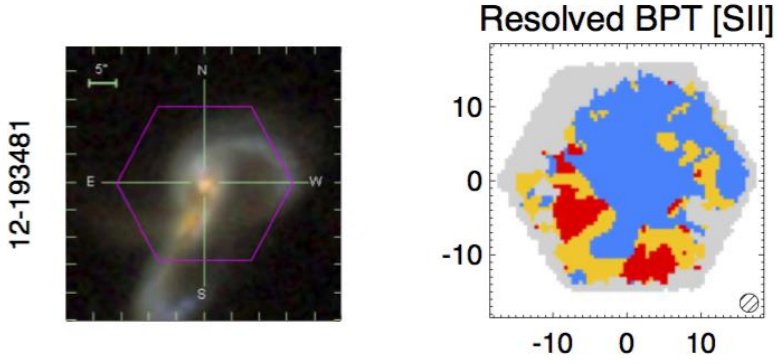

ionoising source of LIERS

- The extra-planar and inter-arm LIER emission in SF galaxies can be identified as diffuse ionised gas(DIG). The source of ionisation of the diffuse ionised gas is still un- clear, however it is likely that escaping hardened radiation from star forming regions contributes to the ionisation budget, with a possible contribution from ionising photons from old stellar populations.

- Post asymptotic giant branch (pAGB) stars have been shown to produce the required hard ionising spectrum necessary to excite LIER emission (Binette et al. 1994; Stasinska et al. 2008) and are thus the ideal candidate to power LIER emission in eLIER and cLIER galaxies.

Diffuse ionized gas(DIG) Zhang et al. 2016

- Due to the limited spatial resolution of MaNGA (2” covers 1 kpc at z=0.025), while the size of a typical H ii region is a few to hundreds of pc. So the light in one spaxel is always a mixture of H ii region emission and the surrounding DIG.
- ΣHα can be used to separate the two different kinds of regions: low ΣHα DIG dominated regions and high ΣHα H ii region dominated regions.

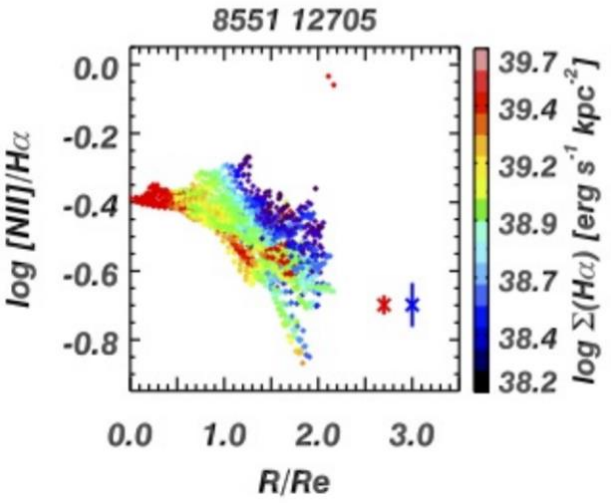

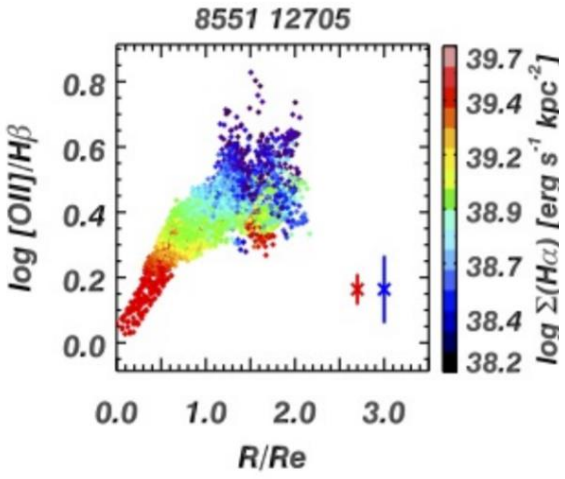

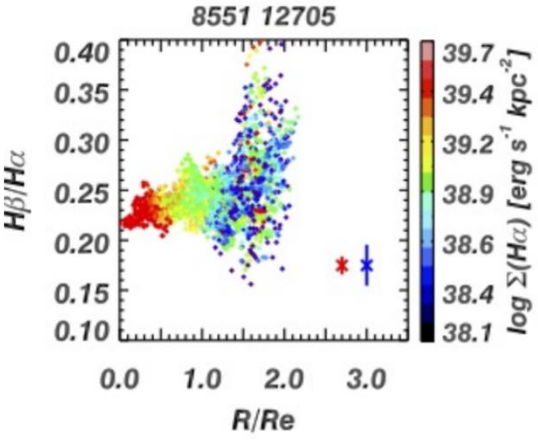

SDSS-IV MaNGA: The Impact of Diffuse Ionized Gas on Emission-line Ratios, Interpretation of Diagnostic Diagrams, and Gas Metallicity Measurements

ABSTRACT

Diffuse Ionized Gas (DIG) is prevalent in star-forming galaxies. Using a sample of 365 nearly face-on star-forming galaxies observed by MaNGA, we demonstrate how DIG in star-forming galaxies impacts the measurements of emission line ratios, hence the interpretation of diagnostic diagrams and gas-phase metallicity measurements. At fixed metallicity, DIG-dominated low $\Sigma_{\mathrm{H}\alpha}$ regions display enhanced [S II]/Hα, [N II]/Hα, [O II]/Hβ, and [O I]/Hα. The gradients in these line ratios are determined by metallicity gradients and $\Sigma_{\mathrm{H}\alpha}$. In line ratio diagnostic diagrams, contamination by DIG moves H II regions towards composite or LI(N)ER-like regions. A harder ionizing spectrum is needed to explain DIG line ratios. Leaky H II region models can only shift line ratios slightly relative to H II region models, and thus fail to explain the composite/LI(N)ER line ratios displayed by DIG. Our result favors ionization by evolved stars as a major ionization source for DIG with LI(N)ER-like emission.

DIG can significantly bias the measurement of gas metallicity and metallicity gradients derived using strong-line methods. Metallicities derived using N2O2 are optimal because they exhibit the smallest bias and error. Using O3N2, R_{23}, N2=[N II]/Hα, and N2S2Hα (Dopita et al. 2016) to derive metallicities introduces bias in the derived metallicity gradients as large as the gradient itself.

The strong-line method of Blanc et al. (2015; IZI hereafter) cannot be applied to DIG to get an accurate metallicity because it currently contains only H II region models which fail to describe the DIG.